New Horizons in Earth Reinforcement – Otani, Miyata & Mukunoki (eds)
© 2008 Taylor & Francis Group, London, ISBN 978-0-415-45775-0

Improvement of earthquake resistance by reinforcing toe of embankments

K. Oda, K. Tokida, Y. Egawa & K. Tanimura
Graduate School of Engineering, Osaka University, Osaka, Japan

ABSTRACT: Recently, the development of economical and effective method for improving the seismic resistance of infrastructures is required strongly. In this paper, the availability of reinforcing the toe of embankment to improvement of seismic resistance of road embankment is discussed through the experiments and analyses. Both centrifuge model tests in the experiments and elasto-pastic finite element analyses in the analyses are carried out. Consequently, the effect of reinforcing the toe of embankment on both seismic resistance of embankment and sliding zone is elucidated.

1 INTRODUCTION

The 2004 Mid Niigata Prefecture Earthquake which was one of the typical near-field earthquakes caused the serious damage to many kinds of infrastructures in the central area of Niigata Prefecture. Especially, a large number of road embankments, which are main road structures in this area, suffered remarkable damage. The damage of road caused the disruption of the road network in this area, so that it was difficult to deal with an emergency and rehabilitation. About 70% of Japanese country is mountainous area. There are a large number of cities, towns and villages in mountainous areas in Japan. Therefore, the aseismic countermeasures for improving the earthquake resistance of road embankments are required to effectively preserve the road network even at an extreme earthquake.

In this paper, the availability of reinforcing the toe of embankments is investigated experimentally and analytically in order to develop efficient and economical techniques for improving the earthquake resistance of embankments. Firstly, the centrifuge model tests are carried out to experimentally demonstrate the improvement of earthquake resistance of embankments. Then, a numerical simulation, in which an elasto-plastic finite element method is applied, is carried out to discuss the applicability of numerical simulation to the sliding failure of embankment. Finally, the availability of reinforcing the toe of embankments to the improvement of earthquake resistance is confirmed. Furthermore, the residual deformation characteristics of embankments, especially, location and volume of sliding surface in the embankments are discussed.

2 TOE REINFORCEMENT

Figure 1 shows schematic diagrams of embankment both without reinforcement and with reinforcement at its toe. The deformation of embankment will be restricted with reinforcing the toe of embankment, so that its seismic resistance will be improved. The advantages of reinforcing the toe of embankments are as follows;

1) The construction of reinforcements can be carried out without suspending the traffic.
2) The sliding zone can decrease, because the substantial height of embankments decreases.

In this paper, the embankments without and with reinforcements are called as “Non-reinforce embankment” and “Reinforce embankment”, respectively.

3 CENTRIFUGE MODEL TEST

Figures 2 & 3 show the outlines of model embankment used in centrifuge model test. The centrifuge model tests were carried out in Shimizu Institute of

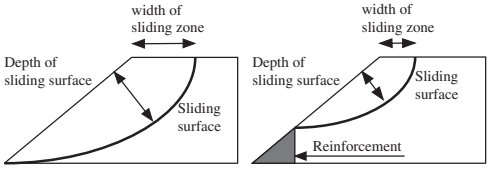

Figure 1. Schematic diagrams of both Non-reinforce and Reinforce embankment.

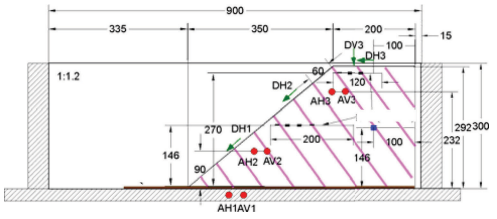

Figure 2. Outline of Non-reinforce embankment model in centrifuge model test.

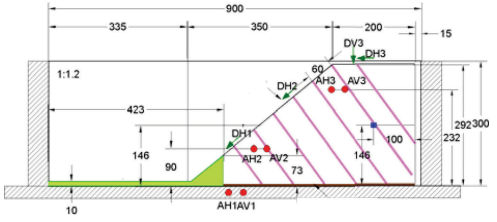

Figure 3. Outline of Reinforce embankment model in centri-fuge test.

Technology. The rigid container used in the centrifuge model test has 900 mm in length, 280 mm in width, and 300 mm in height. The model embankments with a single slope used in the test has 1:1.2 gradients. The centrifuge model tests were carried out under acceleration of 30 g. The model embankments were made of DL clays which were mixed with silicon oil at 5 % of oil content instead of water in order to match viscosity in the model tests to that in the prototype. The average density of DL clay was 1.51 g/cm^3. The shear wave velocity of model embankment under acceleration of 30 g was 175 m/s. An expanded polystyrene board with 15 mm thickness was set between wall and model embankment to absorb the vibration shock from a side wall of the container to model embankment. Silicon greases and rubber membranes were used to decrease the friction between side wall and model embankment. The reinforcement structure at the toe of embankment was made by mixing sand and cement with at the ratio of eight and two in the centrifuge model test. The shear wave velocity of this structure in 1 g field measured by embedded bender elements was 595 m/s. It was considered that the reinforcement structure is stiffer than the embankment body. The reinforcement structure was unified with 10 mm plate which was embedded to the left end of container. Also, the height of reinforcement structure is about quarter of the height of embankment. Therefore, the deformation in the bottom quarter part of Reinforce embankment will be restricted.

The sinusoidal wave as dynamic load was applied to the base of container under acceleration of 30 g. The sinusoidal waves applied were with 60 Hz and 30 cycles. Two types of amplitude of sinusoidal waves,

Table 1. Summary of test results.

	Amplitude	Result
Non-reinforce embankment	300 gal	Fail
Non-reinforce embankment	500 gal	Fail
Reinforce embankment	300 gal	Not fail
Reinforce embankment	500 gal	Fail

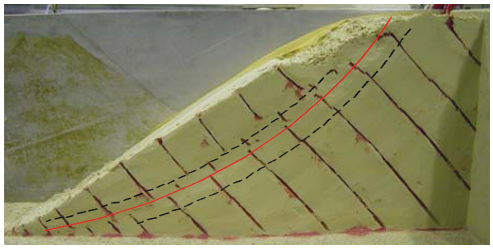

Photograph 1. Residual deformation of Non-reinforce embankment (500 gal).

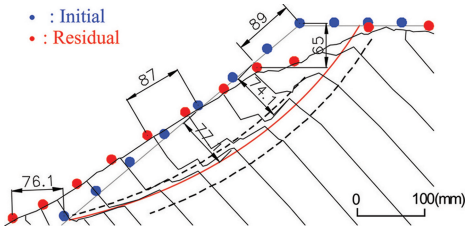

Figure 4. Sketch of residual deformation of Non-reinforce embankment (500 gal).

300 gal and 500 gal, were used in the centrifuge model tests. The accelerations in and to the model embankments were measured through acceleration sensors. Six acceleration sensors were installed as shown in Figures 2 & 3 with AH and AV marks. Also four laser displacement gages as shown in Figures 2 & 3 with DH and DV marks were installed to measure the deformation of the model embankments. Furthermore, the residual deformation in the model embankments were investigated by colored sand as shown in Figures 2 & 3.

Table 1 shows summary of test results. For the Non-reinforce embankments, they failed in the case of attitude of sinusoidal wave of not only 500 gal but also 300 gal. Therefore, the seismic resistance of Non-reinforce embankment might be less than 300 gal. For the Reinforce embankment, the model embankment did not failed in the case of attitude of sinusoidal waves of 300 gal. The seismic resistance of Reinforce embankment might be greater than 300 gal and less than 500 gal. Consequently, the seismic resistance of model embankment could be improved with reinforcing the toe of embankment.

Photograph 1 shows the residual deformation of Non-reinforce embankment in the amplitude of

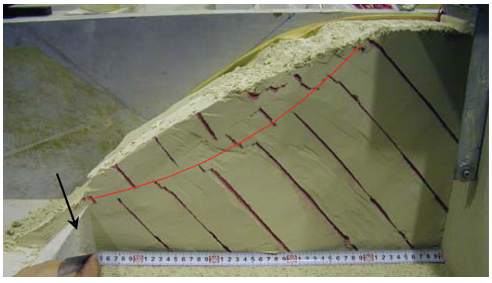

Photograph 2. Residual deformation of Reinforce embankment (500 gal).

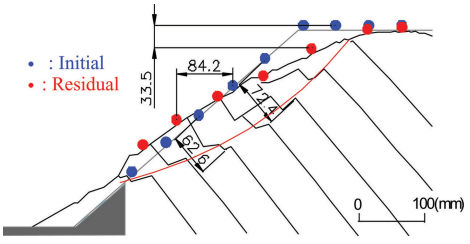

Figure 5. Sketch of residual deformation of Reinforce embankment (500 gal).

sinusoidal wave of 500 gal. Also, Figure 4 illustrates its sketch. Three sliding surfaces could be observed. The middle sliding surface would dominate the sliding failure of this model embankment, based on the displacement of colored sand. The depth of middle sliding surface was about from 70 mm to 80 mm. Also, the width of sliding zone, which is depicted in Figure 1, was about 100 mm. Furthermore, the residual displacement of sliding mass was about from 80 mm to 90 mm.

Photograph 2 shows the residual deformation of Reinforce embankment in the amplitude of sinusoidal wave of 500 gal. Also, Figure 5 illustrates its sketch. A single sliding surface could be observed. The depth of sliding surface was about from 60 mm to 70 mm. Also, the width of sliding zone was about 80 mm. Furthermore, the residual displacement of sliding mass was about from 80 mm to 90 mm. The volume of sliding mass in the Reinforce embankment is less than that in the Non-reinforce embankment. Also, the width of sliding zone in the Reinforce embankment is less than that in the Non-reinforce embankment. That is, the effect of sliding failure of slope on crest of embankment could be reduced. However, the residual displacement of sliding mass could not be shortened.

4 NUMERICAL SIMULATION

The numerical simulation, in which an elasto-plastic finite element method was applied, was carried out to

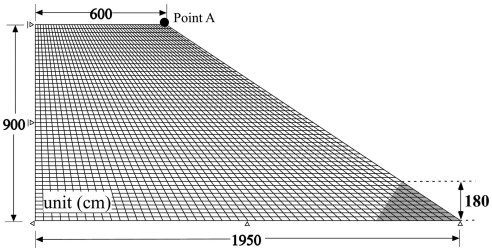

Figure 6. Analytical model used in numerical simulation.

Table 2. Analytical parameters.

a) Embankment body	
Elastic modulus	2.45×10^4kN/m^2
Poisson's ratio	0.25
Cohesion	7.3 kN/m^2
Internal friction angle	36.3°
b) Reinforcement	
Elastic modulus	2.45×10^8kN/m^2
Poisson's ratio	0.25

reproduce the deformation characteristics, especially the seismic intensity and the residual deformation of embankments (Oda et al, 2006). In this analysis, Drucker-Prager criteria is applied as both yield function and plastic potential. In the elasto-plastic calculation, the plastic strain increment is calculated with a return mapping algorithm (Oritz & Simo, 1986) based on non-associated flow role. Also, the spherical arc length procedure proposed by Crisfied (1991), one of the representative displacement control technique is applied, so that the stable numerical calculation can be carried out. In the analysis, firstly, self-weight analysis was carried out to determine the initial stress condition. In this analytical stage, the only vertical body force estimated from unit-weight, is applied in each finite element. Secondly, the horizontal body force increases gradually, so that the bearing resistance of embankments to the horizontal body force reaches to the ultimate state. Finally, the residual deformation in the embankment can be computed.

Figure 6 shows the analytical model used in the numerical simulation. This analytical model was based on the prototype in another series of centrifuge model test (Yoshino, 2006). Table 2 shows analytical parameters used in the numerical simulation. In the numerical simulation, the embankment body and reinforcement bulb were modeled as perfect elasto-plastic and elastic materials, respectively.

Figure 7 shows relationship between horizontal seismic intensity and vertical displacement at the edge of crest of embankment (Point A in Figure 6). The horizontal seismic intensities of Reinforce and Non-reinforce embankment at which the yielding

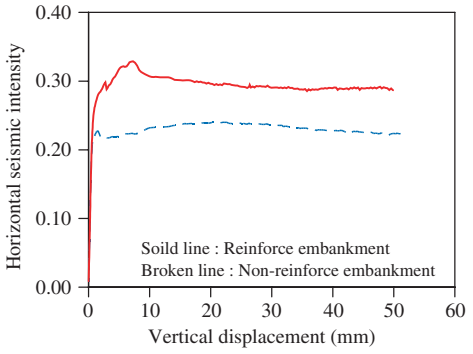

Figure 7. Relationship between horizontal seismic intensity and vertical displacement.

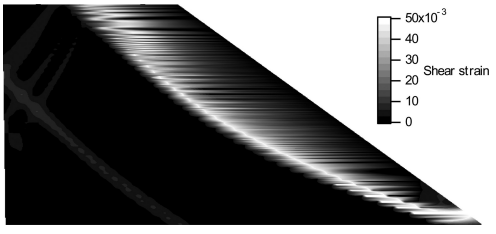

Figure 8. Distribution of shear strain at the final stage in Non-reinforce embankment.

occurs were 0.26 and 0.22, respectively. After the yielding occurred, the horizontal seismic intensity of Non-reinforce embankment hardly varied. On the other hand, that of Reinforce embankment gradually increases with the vertical displacement increasing. The horizontal seismic intensity was at the maximum, 0.33, at the vertical displacement of about 12 mm. Then, it decreased to about 0.30. After that, it hardly varied with the vertical displacement increasing. The horizontal seismic intensity at residual state in Reinforce embankment was about 1.3 times of that in Non-reinforce embankment. As was observed in the centrifuge model test, it was found that the seismic resistance of Reinforce embankment is greater than that of Non-reinforce embankment from the numerical simulation, too.

Figures 8 & 9 show the distribution of shear strain at the final stage of numerical simulation in Non-reinforce embankment and Reinforce embankment, respectively. In each case, a single narrow strap in which a remarkable shear strain occurs was formed. These straps must correspond to the sliding surface. The narrow strap in the Non-reinforce embankment reaches from the toe of embankment to the center of crest. Also, that in the Reinforce embankment reaches from the top of reinforcement bulb to the center of

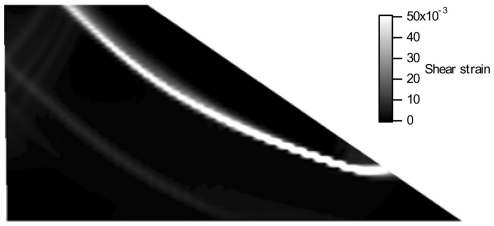

Figure 9. Distribution of shear strain at the final stagte in Reinforce embankment.

crest, because the reinforcement bulb restricts deformation around toe of embankment. Therefore, the volume of sliding mass in the Reinforce embankment was less than that in the Non-reinforce embankment. However, there is little difference of width of sliding zone, which is depicted in Figure 1, between Reinforce and Non-reinforce embankment. The results of numerical simulation did not agree with those of centrifuge model tests. The further research would be required to resolve this difference.

5 CONCLUSIONS

In this paper, the improvement of seismic resistance of embankments by reinforcing their toe was discussed through experiments and numerical analyses. The main conclusions are summarized as follows.

1) The seismic resistance of embankments increases with reinforcing their toe.
2) The volume of sliding mass decreases with reinforcing the toe of embankments.
3) The width of sliding zone in Reinforce embankment is less than that in Non-reinforce embankment in the centrifuge model test.
4) There are little deference of width of sliding zone between Reinforce and Non-reinforce embankment.

REFERENCES

Crisfield, M.A. 1981. A fast incremental/iterative solution proceedure that handles snap through. Com. & Struc. 13, 55–62.

Oritz, M. & Simo, J.C. 1986. An analysis of a new class of integration algorithms for elastoplastic constitutive relations. I.J. Nu. Meth. Eng. 23, 353–366.

Tanimura, K., Oda, K., Tokida, K. & Egawa, Y. 2006. Applicability of elasto-plastic ultimate analysis to performance of road embankment at earthquake. Proc. of the 41th Annual meetings of JGS. 1279–1280.

Yoshino, T., Tokida, K., Nabeshima, Y. Nakahira, A. & Otsuki, A. 2006. Seismic centrifuge model test about slope failure of road embankment. Proc. of the 41th Annual meetings of JGS. 2087–2090.